Published in final edited form as:
Curr Cardiovasc Imaging Rep. 2010 February ; 3(1): 42–49. doi:10.1007/s12410-009-9002-3.

Nanomedicine and Cardiovascular Disease

Jason R. McCarthy
The Center for Molecular Imaging Research and The Center for Systems Biology, Harvard Medical School and Massachusetts General Hospital, 149 13th Street, 6th Floor, Charlestown, MA 02129, USA

Abstract

Nanomedicine has become an important tool in the imaging and therapy of numerous diseases. This is due, in large part, to the ability to generate multifunctional nanoagents bearing combinations of targeting, diagnostic, and therapeutic moieties, allowing for the tailoring of the properties of the synthesized nanomaterials. With respect to cardiovascular disease and its sequelae, nanomedicine has the potential to detect and treat some of the leading causes of death and disability in the developed world, including atherosclerosis, thrombosis, and myocardial infarction. As such, this review focuses on some of the most poignant examples of the utility of nanomedicine in the detection and treatment of cardiovascular disease that have been recently reported.

Keywords

Nanomedicine; Imaging; Therapy; Cardiovascular disease

Introduction

The sequelae of cardiovascular disease are amongst the leading causes of death and disability in the developed world. Thus, much research has been undertaken in order to prevent and treat the resulting cardiovascular syndromes. One greatly enabling technology that has arisen over the past decade is nanomedicine. Although very few nanomaterial-based preparations have made it into clinical use thus far, there are an abundance of data demonstrating the multitude of advantages that this class of agents possesses, including longer circulation times and greater permeability into inflamed tissues.

Nanomaterials are typically defined as those less than 100 nm in diameter, although particles up to 400 nm may demonstrate some enhanced vascular permeability. Depending upon the particle formulation, some materials, such as polymeric nanoparticles or liposomes, are able to encapsulate high payloads of diagnostic or therapeutic moieties, whereas others, such as metal oxides, can be appended with a plethora of functional ligands. The surface modification of nanoparticles also allows for the modulation of their biodistribution, via addition of targeting ligands, such as antibodies, aptamers, peptides, and small molecules. Due to the large surface area–to-volume ratio of nanomaterials, a number of different ligands can be attached, making the agent multi-functional. In particular, theranostic nanoparticles, or those bearing both

The Center for Molecular Imaging Research and The Center for Systems Biology, Harvard Medical School and Massachusetts General Hospital, 149 13th Street, 6th Floor, Charlestown, MA 02129, USA jason_mccarthy@hms.harvard.edu.

Disclosure The author has no relevant affiliations or financial involvement with any organization or entity with a financial interest in or financial conflict with the subject matter or materials discussed in the manuscript. This includes employment, consultancies, honoraria, stock ownership or options, expert testimony, grants or patents received or pending, or royalties.

diagnostic and therapeutic functionalities, can be synthesized, and allow for determination of the localization of the nanoagent concomitant with the treatment of disease.

While this review is not designed to be all encompassing, it highlights some of the most recent nanomedicine-based approaches that have been utilized to image and treat the syndromes resulting from cardiovascular disease, such as atherosclerosis, thrombosis, myocardial infarction (MI), and transplant rejection. More in-depth reviews of the application of nanotechnology in cardiovascular and other diseases can be found elsewhere [1–5].

Nanoparticles in the Detection and Treatment of Atherosclerosis

Of the cardiovascular syndromes, atherosclerosis has received the most attention from nanomedicine researchers. This is likely due to the number of deleterious consequences resulting from the rupture of inflamed, vulnerable plaques. It is also resultant of the number of potential targets within the lesions, including an abundance of specific cell types, such as macrophages, and the upregulation of cell surface receptors, such as vascular cell adhesion molecule-1 (VCAM-1). Clinically, there exists a need to identify vulnerable lesions before the onset of symptoms.

A number of strategies have been investigated for the detection of lesions, such as the fluorescent or radiolabeling of antibodies or other affinity ligands targeted to specific receptors [2,6,7]. With regard to nanoagents, most of the synthesized agents have relied upon the innate uptake of the particles by phagocytic macrophages within the lesions. This is readily exemplified in a number of recent articles by Nahrendorf et al. In their work, the authors utilize epichlorohydrin-crosslinked dextran-coated iron oxide (CLIO) nanoparticles for the targeted imaging of lesions in vivo. In fact, the authors were able to synthesize a multimodal nanoagent capable of detecting atherosclerotic plaques in apolipoprotein E–deficient ($apoE^{-/-}$) mice by fluorescence, magnetic resonance, and nuclear imaging [8•]. To the surface coating of this agent was conjugated a near-infrared fluorophore (VivoTag 680; VisEn Medical, Woburn, MA), as well as diethylenetriaminepentaacetic acid to allow for the coordination of ^{64}Cu. The main advantage of this system is that the detection threshold for positron emission tomography (PET) imaging with ^{64}Cu is 50-fold lower than what is readily detectable by MRI, as determined in phantoms in vitro. When utilized in vivo in atherosclerotic plaque–laden mice, the nanoagent readily accumulated in the aortic arch and root, as determined by PET-CT imaging, with a target-to-background ratio (TBR) of 5.1±0.9, compared with surrounding tissues. The mice were subsequently subjected to MRI, which demonstrated a significant decrease in signal intensity in the aortic root, a phenomenon that is well known for the accumulation of iron oxide nanoparticles. After sacrifice, the aortas of the mice were excised and digested to form a single-cell suspension, which was then labeled with a cocktail of fluorescently labeled antibodies and subject to flow cytometry in order to identify the cell types in which the agent accumulated. As expected, most of the cells that accumulate the nanoagent are monocytes and macrophages (73.9%). Neutrophils (17.2%), endothelial cells (4.2%), smooth muscle cells (0.4%), lymphocytes (4.3%), and other cells (6.6%) took up the remaining agent, although to a lesser degree than macrophages. Encouragingly, iron oxide–based nanosensors have already demonstrated significant utility in the clinical arena (please see the article by Young et al. in this issue of *Current Cardiovascular Imaging Reports*).

The role that protease-activatable nanosensors may play in the detection of atherosclerotic lesions has also been investigated [9]. Three differently sized nanoagents were synthesized (5, 25, and 40 nm) in order to allow for the investigation of the differential localization and activation kinetics of each agent. These nanosensors are fluorogenic in the presence of cathepsin B, a protease that is abundantly expressed by macrophages and monocytes. Initially, the blood half-lives of the respective agents were assayed and demonstrated increased retention

with increasing agent size. The agents were then injected into plaque-laden apoE$^{-/-}$ mice and allowed to circulate for 24 h prior to the mice being sacrificed, and the aortas were excised and imaged by fluorescence reflectance imaging (FRI). The largest agent (40 nm) exhibited the most significant activation within the diseased tissue (TBR of 7.13±1.36), whereas the 5-nm nanoagent exhibited the least (TBR of 4.76±0.56). The utility of the probes was further investigated by hybrid fluorescence-mediated tomography/x-ray CT (FMT-CT) imaging. This allows for the anatomical localization of the fluorescence signal to be determined. As was illustrated ex vivo, the largest probe demonstrated the most significant accumulation within atherosclerotic lesions, especially the aortic root, 24 h after injection, whereas the 5-nm particle had the fastest "wash in" and "wash out" kinetics. The authors further utilized the 40-nm particle to examine the effectiveness of statin therapies in decreasing inflammation, as atorvastatin is known to reduce the recruitment of monocytes, partly through the reduction of VCAM-1 expression. As compared with the control mice that did not receive the statin, the treated mice demonstrated a 2.6-fold decrease in probe signal in the FMT-CT (Fig. 1), which was further correlated with quantitative polymerase chain reaction for expression of cathepsin B.

Fayad and coworkers have also utilized the phagocytic activity of macrophages for the delivery of a novel CT contrast agent to atherosclerotic lesions [10]. This polyiodinated nanoparticle, based upon surfactant-dispersed crystalline ethyl-3,5-bis(acetylamino)-2,4,6-triiodobenzoate (N1177), possessed a mean diameter of 259 nm and resulted in 67 mg of iodine per milliliter of agent. When injected into healthy New Zealand white rabbits, the agent displayed significantly longer retention times than a conventional, clinically used contrast agent (iopamidol), and decreased rapidly by 2 h post-injection. N1177 was next investigated in atherosclerotic lesion–laden rabbits. At 2 h after intravenous injection, where the background signal in the vasculature is expected to be low, accumulation of the agent within macrophage-rich lesions led to significant enhancement of the plaques in the CT images. The authors have recently explored the correlation between the intensity of the CT enhancement of these particles with PET imaging using ^{18}F-FDG, which has shown promise in the imaging of inflamed atherosclerotic lesions [11]. As hypothesized, N1177 accumulation within atherosclerotic lesions corresponded well with the elevated metabolic activity associated with ^{18}F-FDG uptake. These results were further correlated with macrophage burden by immunohistology.

While significant focus has been placed on the imaging of atherosclerotic vascular disease using nanoparticulate agents, researchers are beginning to utilize the platforms already developed for diagnostic applications to co-deliver therapeutics. We have detailed the synthesis of light-activated theranostic nanoparticles for the treatment of atherosclerosis via the focal ablation of inflammatory macrophages [12,13]. These agents, based upon CLIO, contain near-infrared light-activated photosensitizers, as well as near-infrared fluorophores, each at spectrally distinct wavelengths. This allows for the determination of agent localization prior to therapy. In vitro, the agent demonstrated exceptional uptake and cell killing in murine macrophages. Agent localization and therapeutic efficacy were next examined in the carotid artery of 28-week-old apoE$^{-/-}$mice on a high-fat diet. As determined by intravital fluorescence microscopy (IVFM), the nanoagent demonstrated significant accumulation within atherosclerotic lesions. After the initial imaging session, the carotid artery was irradiated with a 650-nm laser, in order to bring about the therapeutic effect, and the mice were allowed to recover. Twenty-four hours later, one cohort of mice was sacrificed for the histological determination of focal cell killing by terminal deoxynucleotidyl transferase nick end-labeling (TUNEL) assay. As compared with the control mice, those that received the agent and light exhibited extensive cell killing within the lesions. One week after the initial imaging session, the other cohort of mice was reinjected with the agent and examined by IVFM. Whereas the control mice demonstrated uptake of the agent within the plaques comparable to the initial

imaging session, there was very little localization to the treated lesions, intimating the elimination of the phagocytic inflammatory cells.

Imaging and Therapy of Thrombosis

Thrombosis underlies a number of cardiovascular syndromes, including MI, stroke, and pulmonary embolism. Clinically, the diagnostic regimen that is utilized for the detection of thromboses consists of Doppler ultrasound, x-ray CT imaging, or MRI. Although these techniques excel at localizing thrombi, they cannot readily characterize clots, including their constituent components or biological age. This type of information would readily assist in the determination of treatment options and their resultant efficacy. Thus, a number of molecular imaging strategies have been developed in order to visualize thrombus formation, including fluorescently labeled platelets [14–17], and fluorescently or radiolabeled ligands targeted to other components of the thrombus, including fibrin [18–21] and coagulation factors [22,23].

We reported the synthesis of two nanoparticulate imaging agents for the simultaneous detection of fibrin and activated factor XIII (FXIIIa) [24]. While fibrin is omnipresent during thrombogenesis, FXIIIa is seen as a hallmark of acute thrombi, as its main function is to stabilize the clot by crosslinking fibrin monomers, as well as covalently conjugating α_2-antiplasmin to the thrombus, making it more resistant to thrombolysis. When used in tandem, imaging agents specific for these two components of thrombi allow for the delineation of the thrombus (via fibrin targeting), as well as the determination of thrombus age (via FXIIIa targeting), and thus lysability. These agents, based upon the CLIO nanoscaffold, were modified with spectrally distinct fluorophores (VivoTag 680 and Cy7), as well as peptide-targeting ligands. The tripeptide sequence Gly-Pro-Arg, which is also the N-terminus of the α-chain of fibrin, has been found to inhibit fibrin and thrombin clotting [25–27]. Subsequent iterations have identified Gly-Pro-Arg-Pro-Pro (GPRPP) as having a highly avid binding affinity for fibrin, to which we have appended the C-terminal sequence GGSKGC, in order to allow for conjugation to CLIO. In order to target FXIIIa, a peptide sequence, GNQEQVSPLTLLKC, originally identified as the N-terminus of α_2-antiplasmin was utilized [22,23]. This peptide is covalently crosslinked into thrombi by FXIIIa via the glutamate residue. When incubated with fresh frozen plasma clots in vitro, the targeted nanoagents readily bound to the clots, as determined by FRI in the respective fluorescence channels, with the fibrin-targeted agent exhibiting TBR of 16.6±1.7, whereas the FXIIIa-targeted agent demonstrated TBR of 30±2.8. The agents were next utilized in a ferric chloride-induced murine model of thrombosis. Thirty minutes after thrombosis, the agents were injected intravenously and were allowed to circulate for an additional 30 minutes, at which time the mouse was sacrificed, and the thrombosed jugular was resected and imaged by FRI. As was demonstrated in vitro, the fibrin-targeted and FXIIIa-targeted agents displayed significant TBR (2.19±0.33 and 26.8±3.2, respectively). Recently, we also demonstrated that these agents are readily amenable to in vivo imaging by intravital confocal microscopy.

Nanomedicine approaches have also been applied to the treatment of thrombosis. Two separate groups have investigated the use of iron oxide nanoparticles for the magnetically targeted delivery of thrombolytics. Magnetic targeting involves the application of a magnetic field to the site of interest, followed by injection of the magnetic nanoparticle preparation. As the agent passes through the circulation, it accumulates within the magnetic field at the target site. Ma et al. [28] synthesized particles coated with polyacrylic acid, to which they covalently conjugated recombinant tissue plasminogen activator (rtPA). Strategically, this is a novel idea, as the main side effect encountered when using plasminogen activators is intracerebral hemorrhage (ICH), and attachment to a magnetic nanoparticulate scaffold may enhance retention at the target site and diminish the occurrence of ICH. As compared with free rtPA, the conjugated derivative exhibited equivalent fibrinolytic efficacy and amidolytic activity in

vitro. When utilized in vivo in a rat hind limb ischemia model, the thrombolytic conjugate demonstrated fivefold more thrombolytic efficacy than free rtPA, while under magnetic targeting. In the absence of a magnet, the conjugate did not demonstrate appreciable thrombolysis.

A similar approach was also utilized by Bi et al. [29], in which they conjugated urokinase (UK) to an amine-modified dextran-coated magnetic nanoparticle. The UK was conjugated to the particle after modification of the dextran coating with glutaraldehyde. The authors tested the resulting nanoagent in a shunt model, in which the right carotid artery and left jugular vein of Sprague-Dawley rats were directly connected by polyethylene tubing containing silk thread, on which the thrombus would form. Fifteen minutes after thrombus formation, the rats received saline, UK, the nanoparticle conjugate, or the nanoparticle conjugate under magnetic targeting, which was allowed to circulate for 30 minutes, at which time the silk thread was removed in order to determine residual thrombus weight. While all therapeutic interventions resulted in a decrease in thrombus size, as compared with saline, magnetic targeting resulted in fivefold more efficacy than UK and was 2.6-fold more effective than the nontargeted particle. Additionally, the researchers examined the residual fibrinogen in circulation, as well as the bleeding times, in which the magnetic targeting of the nanoagent significantly decreased the systemic activation of plasminogen, thereby minimizing increases in bleeding times.

Imaging Inflammation in MI

MI brings about a massive inflammatory response characterized by the recruitment of neutrophils and macrophages to the damaged myocardium. This response is sequential and results in the healing of the infarct. Recruited leukocytes secrete a number of proteinases, such as matrix metalloproteinases, and proteases, such as cathepsin B, in order to facilitate the clearing away of necrotic debris. Efficient repair of the myocardium is subsequently completed by the deposition of new tissues and remodeling. If this healing is inadequate, it may eventually lead to rupture of the infarct and heart failure. The sequential nature of this process has allowed for the design of a number of probes to image the resulting inflammatory response.

Sosnovik et al. [30] previously demonstrated that the recruitment of phagocytic macrophages to MI can be visualized in vivo by both FMT and MRI using multimodal magnetofluorescent nanoparticles, detailed above. Nahrendorf et al. [31] built upon this initial work and were able to additionally examine the proteolytic activity of the macrophages and neutrophils using an enzyme-activated fluorogenic probe for cathepsins. This protocol allows for functional examination of cellular and molecular events governing the healing process. The authors were also able to investigate impaired infarct healing in a knockout model, in which leukocyte recruitment is impaired. As compared with the wild-type animal, the knockout demonstrated greatly reduced phagocytic potential, as well as decreased cathepsin B probe activation.

One additional species that is introduced into the damaged myocardium by leukocytes is myeloperoxidase (MPO). MPO is an enzyme that is present within these phagocytic cells in order to provide for microbicidal and viricidal properties. In the presence of chloride ions, MPO catalyzes the formation of hypochlorous acid (HOCl) from hydrogen peroxide, in addition to a number of other reactive species, such as hydroxyl radicals, chloramines, tyrosyl radicals, and nitrogen dioxide. MPO is implicated in the initiation or progression of a number of diseases, including atherosclerosis and cancer. The utility of an activatable MRI contrast agent for the detection of MPO in healing infarcts has previously been reported [32]. This agent, which contains a gadolinium chelate, polymerizes upon oxidation, causing a significant increase in T_1 relaxation, which is readily imaged by MRI. When injected into mice with MI, the agent readily delineated the infarct.

Recently, we described the synthesis and utility of a highly selective far-red emissive fluorogenic nanoagent that is activated by HOCl and peroxynitrite [33•]. This probe, based upon the modification of CLIO with an activatable oxazine-based dye, demonstrated a 500-fold activation in vitro when treated with HOCl. When incubated with flow-sorted neutrophils isolated from pure mouse blood, the probe demonstrated significant fluorescence within the cells, as determined by flow cytometry. The nanoagent was subsequently tested in vivo in mice bearing MI. The probe was injected intravenously 12 to 14 h after MI, and was imaged at 24 h after injection, in order to allow for maximum neutrophil accumulation at the site of the insult. When examined by FRI, the infarcted hearts demonstrated significant fluorescence accumulation within the infarcted region, compared with mice that were not given an MI or mice that received the free oxazine dye not bound to the nanoparticulate platform (Fig. 2). While the utility of this nanoagent was demonstrated in MI, it may also enable the detection of inflammation in atherosclerosis, cancer, metastasis, and organ rejection.

Nanoagents for Use in the Detection of Transplant Rejection

Clinically, patients who have undergone heart transplantation must partake in repeated endomyocardial biopsy in order to detect transplant rejection. This procedure requires catheterization, entails significant risks, and is prone to sampling errors, especially over the lifetime of the patient as fibrotic tissue builds where the biopsies have been removed. An alternate strategy for monitoring rejection, based upon the noninvasive detection of macrophage infiltration and protease activity, has recently been investigated by a group led by Dr. Peter Libby [34••]. In these experiments, mice were heterotopically transplanted with isografts (B/6 to B/6) or allografts (Balb/C to B/6) in order to examine the sequence of inflammatory cell accumulation, and subsequently the degree of macrophage and cathepsin-releasing cell infiltration. The isografts allow for a control for the non-immunological parenchymal damage caused by periods of warm and cold ischemia. Histological examination of the grafted hearts has revealed that whereas neutrophil localization is relatively low, macrophages, amplifiers of T-cell–driven response in graft rejection, accumulated significantly in the allografts by day 7 post-transplant. Not surprisingly, CD4 and CD8 T lymphocytes also accumulated within the grafts. In order to investigate the in vivo imaging of transplant rejection, the authors utilized magnetofluorescent CLIO as a marker of phagocytic activity, and ProSense-680 (VisEn Medical) as a nanoconstruct for the determination of cathepsin activity. Prosense is a fluorogenic particle that is activated by cleavage with cathepsins. Initial in vivo experimentation determined that both CLIO and ProSense displayed significant accumulation within macrophages as assayed by immunohistochemistry, as well as by flow cytometric examination of the digested donor hearts. In vivo imaging of transplant rejection was accomplished by FMT, which displayed significantly higher signal from both nanoprobes in the allograft hearts, as opposed to the isografts (Fig. 3). Additionally, because CLIO can also serve as a magnetic resonance contrast agent, accumulation was also investigated by MRI, which correlated well with the FMT results. While these results are indeed promising for the detection of acute transplant rejection, the technique is severely limited by the clinical feasibility of FMT, although a number of groups are currently investigating novel catheter designs that will allow for intravascular fluorescence imaging.

Conclusions

Nanomedicine allows for the creation of agents specifically designed to enhance the diagnosis and treatment of disease. With regard to cardiovascular disease, nanoagents have found applicability in a wide range of disorders, although very few have transitioned to the clinic. Given the rapid advances in nanoagent synthesis and utility, clinical application of these technologies can be anticipated in the near term.

References

Papers of particular interest, published recently, have been highlighted as:

• Of importance

•• Of major importance

1. Cormode DP, Skajaa T, Fayad ZA, Mulder WJ. Nanotechnology in medical imaging: probe design and applications. Arterioscler Thromb Vasc Biol 2009;29:992–1000. [PubMed: 19057023]
2. Jaffer FA, Libby P, Weissleder R. Optical and multimodality molecular imaging: insights into atherosclerosis. Arterioscler Thromb Vasc Biol 2009;29:1017–1024. [PubMed: 19359659]
3. McCarthy JR, Kelly KA, Sun EY, Weissleder R. Targeted delivery of multifunctional magnetic nanoparticles. Nanomed 2007;2:153–167.
4. McCarthy JR, Weissleder R. Multifunctional magnetic nanoparticles for targeted imaging and therapy. Adv Drug Deliv Rev 2008;60:1241–1251. [PubMed: 18508157]
5. Skajaa T, Cormode DP, Falk E, et al. High-Density Lipoprotein-Based Contrast Agents for Multimodal Imaging of Atherosclerosis. Arterioscler Thromb Vasc Biol. 2009 In press.
6. Nahrendorf M, Sosnovik DE, French BA, et al. Multimodality cardiovascular molecular imaging, Part II. Circ Cardiovasc Imaging 2009;2:56–70. [PubMed: 19808565]
7. Sinusas AJ, Bengel F, Nahrendorf M, et al. Multimodality cardiovascular molecular imaging, part I. Circ Cardiovasc Imaging 2008;1:244–256. [PubMed: 19808549]
8 •. Nahrendorf M, Zhang H, Hembrador S, et al. Nanoparticle PET-CT imaging of macrophages in inflammatory atherosclerosis. Circulation 2008;117:379–387. [PubMed: 18158358] The trimodal nanoagent utilized in this study was able to correlate macrophage burden with PET signal. It was also able to demonstrate localization to atherosclerotic lesions by both MRI and fluorescence imaging.
9. Nahrendorf M, Waterman P, Thurber G, et al. Hybrid in vivo FMT-CT imaging of protease activity in atherosclerosis with customized nanosensors. Arterioscler Thromb Vasc Biol 2009;29:1444–1451. [PubMed: 19608968]
10. Hyafil F, Cornily JC, Feig JE, et al. Noninvasive detection of macrophages using a nanoparticulate contrast agent for computed tomography. Nat Med 2007;13:636–641. [PubMed: 17417649]
11. Hyafil F, Cornily JC, Rudd JH, et al. Quantification of inflammation within rabbit atherosclerotic plaques using the macrophage-specific CT contrast agent N1177: a comparison with 18F-FDG PET/CT and histology. J Nucl Med 2009;50:959–965. [PubMed: 19443582]
12. McCarthy, JR.; Jaffer, FA.; Weissleder, R. Imaging and therapy of atherosclerotic lesions with theranostic nanoparticles. In: Rege, K.; Medintz, IL., editors. Methods in Bioengineering: Nanoscale Bioengineering and Nanomedicine. Artec House; Boston: 2009. p. 137-151.
13. McCarthy JR, Jaffer FA, Weissleder R. A macrophage-targeted theranostic nanoparticle for biomedical applications. Small 2006;2:983–987. [PubMed: 17193154]
14. Flaumenhaft R, Tanaka E, Graham GJ, et al. Localization and quantification of platelet-rich thrombi in large blood vessels with near-infrared fluorescence imaging. Circulation 2007;115:84–93. [PubMed: 17179017]
15. Frenette PS, Johnson RC, Hynes RO, Wagner DD. Platelets roll on stimulated endothelium in vivo: an interaction mediated by endothelial P-selectin. Proc Natl Acad Sci U S A 1995;92:7450–7454. [PubMed: 7543682]
16. Massberg S, Sausbier M, Klatt P, et al. Increased adhesion and aggregation of platelets lacking cyclic guanosine 3′,5′-mono-phosphate kinase I. J Exp Med 1999;189:1255–1264. [PubMed: 10209042]
17. Sim DS, Merrill-Skoloff G, Furie BC, et al. Initial accumulation of platelets during arterial thrombus formation in vivo is inhibited by elevation of basal cAMP levels. Blood 2004;103:2127–2134. [PubMed: 14645013]
18. Balasubramanian V, Grabowski E, Bini A, Nemerson Y. Platelets, circulating tissue factor, and fibrin colocalize in ex vivo thrombi: real-time fluorescence images of thrombus formation and propagation under defined flow conditions. Blood 2002;100:2787–2792. [PubMed: 12351386]

19. Falati S, Gross P, Merrill-Skoloff G, et al. Real-time in vivo imaging of platelets, tissue factor and fibrin during arterial thrombus formation in the mouse. Nat Med 2002;8:1175–1181. [PubMed: 12244306]
20. Knight LC, Maurer AH, Ammar IA, et al. Evaluation of indium-111-labeled anti-fibrin antibody for imaging vascular thrombi. J Nucl Med 1988;29:494–502. [PubMed: 3351604]
21. Stratton JR, Cerqueira MD, Dewhurst TA, Kohler TR. Imaging arterial thrombosis: comparison of technetium-99 m-labeled monoclonal antifibrin antibodies and indium-111-platelets. J Nucl Med 1994;35:1731–1737. [PubMed: 7965148]
22. Jaffer FA, Tung CH, Wykrzykowska JJ, et al. Molecular imaging of factor XIIIa activity in thrombosis using a novel, near-infrared fluorescent contrast agent that covalently links to thrombi. Circulation 2004;110:170–176. [PubMed: 15210587]
23. Tung CH, Ho NH, Zeng Q, et al. Novel factor XIII probes for blood coagulation imaging. Chembiochem 2003;4:897–899. [PubMed: 12964167]
24. McCarthy JR, Patel P, Botnaru I, et al. Multimodal nanoagents for the detection of intravascular thrombi. Bioconjug Chem 2009;20:1251–1255. [PubMed: 19456115]
25. Aruva MR, Daviau J, Sharma SS, Thakur ML. Imaging thromboembolism with fibrin-avid 99mTc-peptide: evaluation in swine. J Nucl Med 2006;47:155–162. [PubMed: 16391200]
26. Kawasaki K, Miyano M, Hirase K, Iwamoto M. Amino acids and peptides. XVIII. Synthetic peptides related to N-terminal portion of fibrin alpha-chain and their inhibitory effect on fibrinogen/thrombin clotting. Chem Pharm Bull (Tokyo) 1993;41:975–977. [PubMed: 8339344]
27. Thakur ML, Pallela VR, Consigny PM, et al. Imaging vascular thrombosis with 99mTc-labeled fibrin alpha-chain peptide. J Nucl Med 2000;41:161–168. [PubMed: 10647619]
28. Ma YH, Wu SY, Wu T, et al. Magnetically targeted thrombolysis with recombinant tissue plasminogen activator bound to poly-acrylic acid-coated nanoparticles. Biomaterials 2009;30:3343–3351. [PubMed: 19299010]
29. Bi F, Zhang J, Su Y, et al. Chemical conjugation of urokinase to magnetic nanoparticles for targeted thrombolysis. Biomaterials 2009;30:5125–5130. [PubMed: 19560812]
30. Sosnovik DE, Nahrendorf M, Deliolanis N, et al. Fluorescence tomography and magnetic resonance imaging of myocardial macrophage infiltration in infarcted myocardium in vivo. Circulation 2007;115:1384–1391. [PubMed: 17339546]
31. Nahrendorf M, Sosnovik DE, Waterman P, et al. Dual channel optical tomographic imaging of leukocyte recruitment and protease activity in the healing myocardial infarct. Circ Res 2007;100:1218–1225. [PubMed: 17379832]
32. Nahrendorf M, Sosnovik D, Chen JW, et al. Activatable magnetic resonance imaging agent reports myeloperoxidase activity in healing infarcts and noninvasively detects the antiinflammatory effects of atorvastatin on ischemia-reperfusion injury. Circulation 2008;117:1153–1160. [PubMed: 18268141]
33 •. Panizzi P, Nahrendorf M, Wildgruber M, et al. Oxazine conjugated nanoparticle detects in vivo hypochlorous acid and peroxynitrite generation. J Am Chem Soc 2009;131:15739–15744. [PubMed: 19817443] This is the first example of a long circulating nanoparticulate construct for the detection of MPO activity in vivo. Although used in MI, this probe will demonstrate utility in a number of conditions with inflammatory components, such as atherosclerosis, diabetes, and cancer.
34 ••. Christen T, Nahrendorf M, Wildgruber M, et al. Molecular imaging of innate immune cell function in transplant rejection. Circulation 2009;119:1925–1932. [PubMed: 19332470] This article establishes that the detection of transplant rejection need not be an invasive procedure. Instead, noninvasive determination of macrophage infiltration may serve a diagnostic/prognostic role.

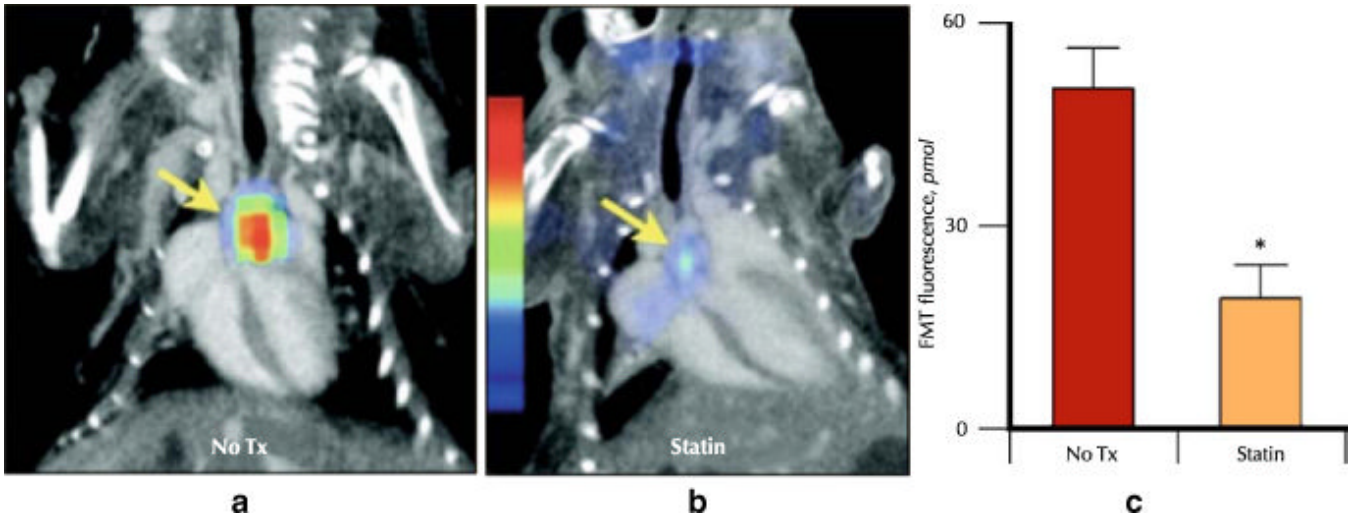

Fig. 1.

The protease sensor with the highest sensitivity, the 40-nm agent, was used in a therapy trial to investigate its potential as a noninvasive imaging biomarker in drug development. **a** and **b**, Fluorescence-mediated tomography (FMT)–CT datasets in respective treatment groups. **c**, Fluorescence activity in the aortic root measured by FMT, 24 h after injection. The protease sensor detected effects of atorvastatin treatment. *Asterisk* indicates $P<0.05$. (*From* Nahrendorf et al. [9]; with permission.)

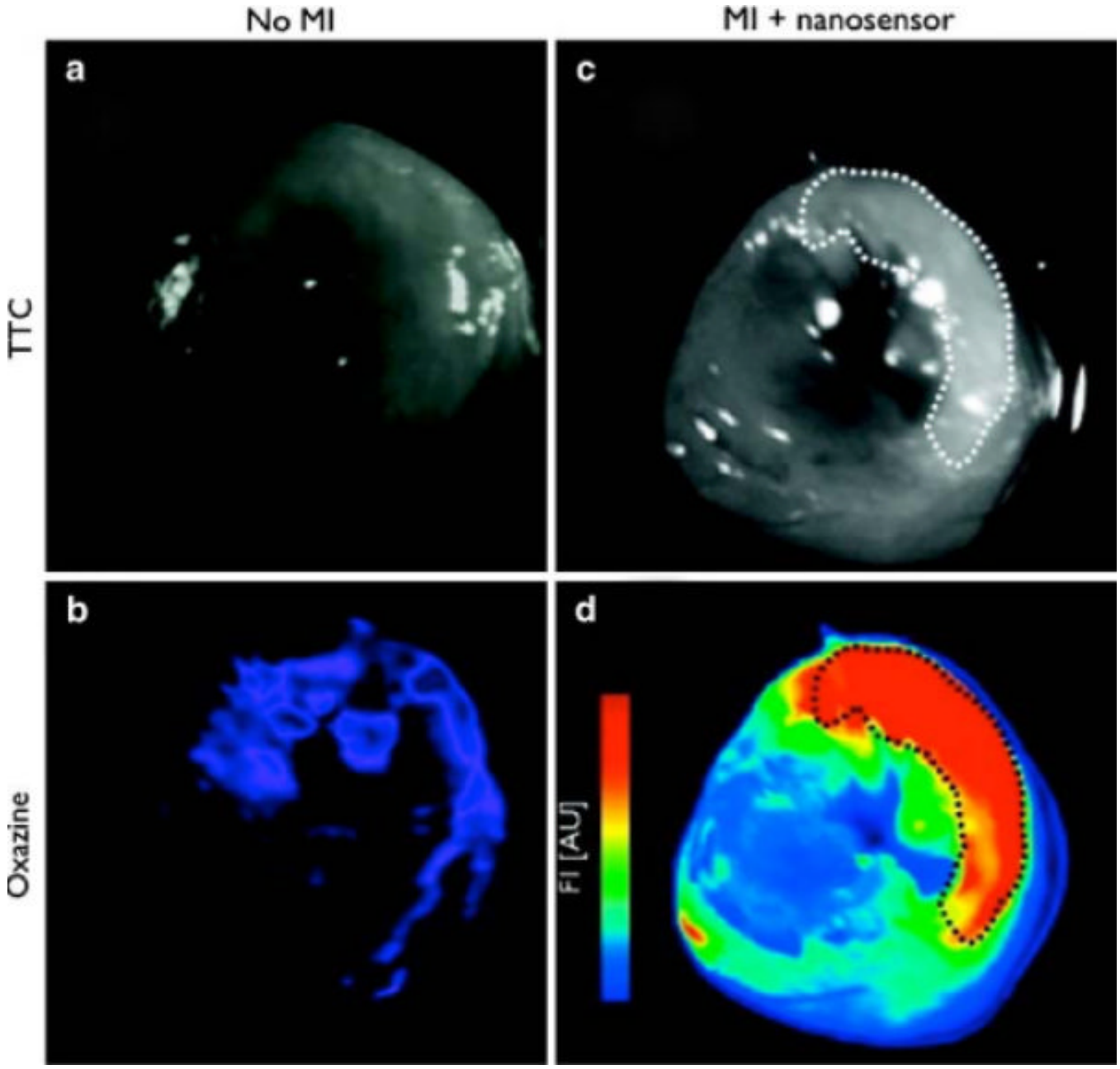

Fig. 2.

Ex vivo fluorescence reflectance imaging comparison of reactive oxygen species sensor localization in wild-type (*left column*) and infarcted mouse hearts (*right*). White light images of triphenyltetrazolium chloride (TTC)–stained heart slices are shown **a**, **c**, with infarcted region highlighted by the *dashed line* throughout. Accumulation of the activated oxazine probe is detectable in the Cy5 channel **b**, **d** [33•]. MI—myocardial infarction

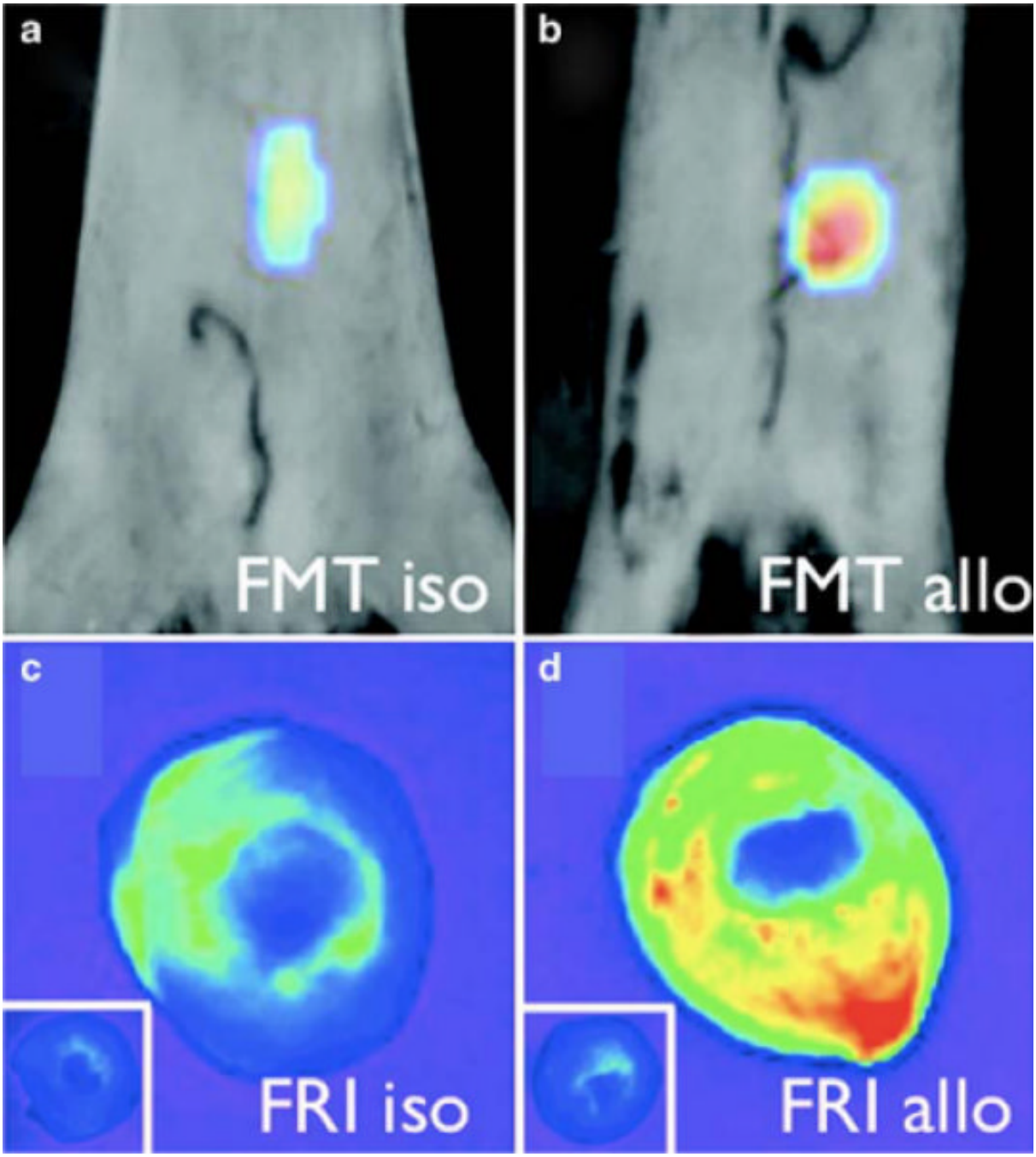

Fig. 3.
In vivo fluorescence-mediated tomography (FMT) demonstrates higher protease activity in the allograft **b** than in the isograft **a** of mice injected with protease sensor. **c** and **d**, The fluorescence signal was further correlated ex vivo by fluorescence reflectance imaging (FRI). (*From* Christen et al. [34••]; with permission.)